

ANESTHESIOLOGY

Constrained Functional Connectivity Dynamics in Pediatric Surgical Patients Undergoing General Anesthesia

Michael P. Puglia II, M.D., Ph.D., Phillip E. Vlisides, M.D., Chelsea M. Kaplan, Ph.D., Elizabeth S. Jewell, M.S., Megan Therrian, B.S., George A. Mashour, M.D., Ph.D., Duan Li, Ph.D.

ANESTHESIOLOGY 2022; 137:28–40

EDITOR'S PERSPECTIVE

What We Already Know about This Topic

- Patterns of connectivity between different brain regions (functional connectivity) undergo structured shifts during stable general anesthesia
- However, in the developing brain, the presence of these connectivity patterns and how they may change across time have not been investigated

What This Article Tells Us That Is New

- During the stable maintenance phase of general anesthesia, functional connectivity patterns in the developing brain are relatively static, in contrast to the dynamic structured transitions previously shown in adults
- Using conventional methods to measure functional connectivity, the developing brain demonstrated a hyperconnected frontal cortex during the loss of consciousness, maintenance, and emergence periods
- This was most marked for frequencies less than 14 Hz and between the prefrontal and frontal regions

ABSTRACT

Background: Functional connectivity in cortical networks is thought to be important for consciousness and can be disrupted during the anesthetized state. Recent work in adults has revealed dynamic connectivity patterns during stable general anesthesia, but whether similar connectivity state transitions occur in the developing brain remains undetermined. The hypothesis was that anesthetic-induced unconsciousness is associated with disruption of functional connectivity in the developing brain and that, as in adults, there are dynamic shifts in connectivity patterns during the stable maintenance phase of general anesthesia.

Methods: This was a preplanned analysis of a previously reported single-center, prospective, cross-sectional study of healthy (American Society of Anesthesiologists status I or II) children aged 8 to 16 yr undergoing surgery with general anesthesia ($n = 50$) at Michigan Medicine. Whole-scalp (16-channel), wireless electroencephalographic data were collected from the preoperative period through the recovery of consciousness. Functional connectivity was measured using a weighted phase lag index, and discrete connectivity states were classified using cluster analysis.

Results: Changes in functional connectivity were associated with anesthetic state transitions across multiple regions and frequency bands. An increase in prefrontal–frontal alpha (median [25th, 75th]; baseline, 0.070 [0.049, 0.101] vs. maintenance 0.474 [0.286, 0.606]; $P < 0.001$) and theta connectivity (0.038 [0.029, 0.048] vs. 0.399 [0.254, 0.488]; $P < 0.001$), and decrease in parietal–occipital alpha connectivity (0.171 [0.145, 0.243] vs. 0.089 [0.055, 0.132]; $P < 0.001$) were among those with the greatest effect size. Contrary to the hypothesis, connectivity patterns during the maintenance phase of general anesthesia were dominated by stable theta and alpha prefrontal–frontal and alpha frontal–parietal connectivity and exhibited high between-cluster similarity ($r = 0.75$ to 0.87).

Conclusions: Changes in functional connectivity are associated with anesthetic state transitions but, unlike in adults, connectivity patterns are constrained during general anesthesia in late childhood and early adolescence.

(*ANESTHESIOLOGY* 2022; 137:28–40)

Understanding changes in neural activity across anesthetic state transitions in children is of high clinical and scientific importance. Clinically, despite the approximately 3.9 million surgeries performed on children annually in the

This article is featured in "This Month in Anesthesiology," page A1. This article is accompanied by an editorial on p. 4. Supplemental Digital Content is available for this article. Direct URL citations appear in the printed text and are available in both the HTML and PDF versions of this article. Links to the digital files are provided in the HTML text of this article on the Journal's Web site (www.anesthesiology.org). This article has a video abstract. This article has a visual abstract available in the online version.

Submitted for publication December 3, 2021. Accepted for publication March 25, 2022. Published online first on April 1, 2022.

Michael P. Puglia II, M.D., Ph.D.: Department of Anesthesiology and Center for Consciousness Science, University of Michigan Medical School, Ann Arbor, Michigan.

Phillip E. Vlisides, M.D.: Department of Anesthesiology and Center for Consciousness Science, University of Michigan Medical School, Ann Arbor, Michigan.

Chelsea M. Kaplan, Ph.D.: Department of Anesthesiology, University of Michigan Medical School, Ann Arbor, Michigan.

Elizabeth S. Jewell, M.S.: Department of Anesthesiology, University of Michigan Medical School, Ann Arbor, Michigan.

Megan Therrian, B.S.: Department of Anesthesiology, University of Michigan Medical School, Ann Arbor, Michigan.

George A. Mashour, M.D., Ph.D.: Department of Anesthesiology, Center for Consciousness Science, and Neuroscience Graduate Program, University of Michigan Medical School, Ann Arbor, Michigan.

Duan Li, Ph.D.: Department of Anesthesiology and Center for Consciousness Science, University of Michigan Medical School, Ann Arbor, Michigan.

Copyright © 2022, the American Society of Anesthesiologists. All Rights Reserved. *Anesthesiology* 2022; 137:28–40. DOI: 10.1097/ALN.0000000000004221

United States alone, there is no validated monitor for the brain to guide perioperative care.¹ Scientifically, there remains an incomplete understanding of the neurobiological correlates of consciousness and developmental neurophysiology.

Although there are many approaches to investigating neural activity across states of consciousness, one that has received particular attention over the past decade is functional connectivity, broadly defined as the statistical covariation between two brain signals. Changes in functional connectivity have been explored as an index for anesthetic state transitions and have been shown to discriminate between anesthetic-mediated changes in states of consciousness.^{2–5} Additionally, functional connectivity has been postulated to represent a potential mechanism for information sharing and integration required for conscious processing.^{2–9} The majority of functional connectivity studies across states of consciousness have been performed in adult subjects, but a recent study in infants demonstrated reduced functional connectivity during the maintenance phase of general anesthesia compared to emergence.⁴ Additionally, studies of functional connectivity often select a specific time period to analyze across states, for example a 100-s epoch during general anesthesia *versus* a 100-s epoch during emergence in the above pediatric study.⁴ Although important, these studies are limited by the measurement of functional connectivity at a single time epoch. More recently, investigation in adults found that functional connectivity patterns underwent structured transitions across time (*i.e.*, dynamic shifts) during the course of stable general anesthesia.^{7,8,10} The finding that the connectivity patterns underwent dynamic shifts during “real-world” surgical anesthesia was also supported by a study of subjects with rigorously controlled surgical levels of general anesthesia without a surgical stimulus.^{7,8} However, whether dynamic connectivity patterns occur in anesthetized children or change during development is unknown.

The primary objectives of this study in children ages 8 to 16 yr were to (1) determine whether measures of functional connectivity reflect anesthetic-induced changes in levels of consciousness and (2) identify temporal dynamics of functional connectivity patterns during surgical anesthesia. As a secondary objective, we aimed to test age-related differences in functional connectivity transitions during general anesthesia, complementing previous work in adult subjects.^{7,8,10} We hypothesized that changes in functional connectivity patterns reflect anesthetic-induced changes in states of consciousness and that, similar to studies in adults, the patterns would undergo dynamic shifts during the stable maintenance phase of general anesthesia.

Materials and Methods

This was a prospective, single-center, cross-sectional, observational study in children undergoing general anesthesia for elective outpatient surgery at C.S. Mott Children’s Hospital, Michigan Medicine (Ann Arbor, Michigan). Recruitment

took place from November 2018 to March 2020. The study was approved by the University of Michigan Medical School Institutional Review Board (Ann Arbor, Michigan; approval No. HUM00142298). Written informed consent was obtained by parents/guardians and verbal or written assent by pediatric patients were obtained before study enrollment. This study adheres to the Strengthening of Reporting of Observational Studies in Epidemiology (STROBE) guidelines¹¹ and was a preplanned substudy of a previously analyzed cross-sectional study of cortical complexity during the perioperative period.¹² Statistical and data analysis plans were defined *a priori* and written and filed with a private entity. Instances where *post hoc* analyses were performed are clearly identified.

Study Population

Pediatric patients (8 to 16 yr old) with American Society of Anesthesiologists (ASA) physical status I or II who were scheduled for outpatient elective surgery with general anesthesia were selected for enrollment. This population was chosen for the following reasons: first, this is a period of massive developmental brain network change¹³; second, this population is compliant with baseline assessment before general anesthesia; and third, adolescence is a relatively understudied age period. An additional inclusion criterion was the planned use of a halogenated ether as the primary anesthetic maintenance agent. Exclusion criteria included a patient history of developmental delay, seizure disorder, neurologic disease, current use of stimulant medications (*e.g.*, amphetamine, dextroamphetamine), head or neck surgery (which might preclude neurophysiologic monitoring), history or suspicion of a difficult airway, physical characteristics that interfere with electrode contact with the scalp, enrollment in conflicting research protocol, or where English was not the primary language.

Anesthetic and Perioperative Management

The goal of this study was to determine changes in functional connectivity across the perioperative period in a real-world setting. As such, no protocol was implemented for altering patient care. Care teams were blinded to the electroencephalogram data to prevent additional sources of bias.

Electroencephalographic Data Acquisition

Electroencephalogram data were recorded as previously described from 16 Ag/AgCl scalp electrodes using a Cognionics (USA) Mobile-128 wireless system and applied based on the international 10 to 20 system.¹² Briefly, after ensuring proper cap size (EASYCAP; Germany), placement was based on electrode position Cz, which was localized to 50% of the distance between the nasion and inion and the preauricular notch measurements. Recordings were sampled at 500 samples/s and referenced to the mastoid. Electrode impedances were monitored continuously and

maintained less than 100 k Ω per the manufacturer's recommendations. Electroencephalographic signals were exported to MATLAB (version R2019b; MathWorks, Inc., USA) and downsampled to 250 Hz. The 60-Hz power-line interference, if present, was removed using multitaper regression technique and Thomas F-statistics implemented in CleanLine plugin for the EEGLAB toolbox.¹⁴

Epoch Selection and Preprocessing

Study epochs selected for analysis are shown in figure 1. Baseline electroencephalogram data ($n = 50$; 4.88 ± 0.39 min; 15 to 16 channels) were recorded in the preoperative eyes-closed resting state before any perioperative medication administration. Loss of consciousness data ($n = 50$; 4.71 ± 0.61 min; 11 to 16 channels) were selected immediately after clinical loss of responsiveness indicated by the clinical provider. Maintenance data ($n = 49$; 5 min; 14 to 16 channels) were selected during the maintenance phase of general anesthesia approximately halfway between the surgical incision and cessation of the anesthetic with adjustment to meet the following criteria: stable age-adjusted minimum alveolar concentration value (greater than 0.7 and less than $\pm 0.1\%$ change) and data suitable for analysis (*i.e.*, free from artifact by visual inspection). Sevoflurane was the most commonly used anesthetic for maintenance ($n = 24$), followed by isoflurane ($n = 15$), then isoflurane supplemented with nitrous oxide ($n = 6$), and sevoflurane supplemented with nitrous oxide ($n = 5$). Emergence data ($n = 45$; 4.28 ± 0.78 min; 9 to 16 channels) were selected 5 min immediately before clinical recovery assessed *via* a validated pediatric sedation assessment tool (University of Michigan Sedation Scale score of 0 to 1).¹⁵ Recovery data ($n = 45$; 3.06 ± 1.21 min; 11 to 16 channels) were recorded

in the eyes-closed resting state immediately after achieving a University of Michigan Sedation Scale score of 0 to 1. One patient was excluded from analysis due to a minimum alveolar concentration below selection criteria in the maintenance phase, and five patients were excluded in the emergence and recovery phase due to data loss (*e.g.*, associated with emergence delirium and electrode displacement).

Electroencephalogram signals were preprocessed as previously described.⁷ First, bad channels and noisy time segments with obvious artifacts were rejected by visual inspection. Second, the signals were detrended using a local linear regression method with a 10-s window at a 5-s step size in the Chronux analysis toolbox¹⁶ and low-pass-filtered at 50 Hz using the `eegfiltnew` function in the EEGLAB toolbox.¹⁴ Third, the signals underwent independent component analysis using the extended-Infomax algorithm in EEGLAB toolbox.¹⁴ Independent components representing cardiac, eye, muscle, or other transient artifacts were identified and removed using visual inspection of the time-domain waveform, power spectrum, and spatial scalp topography. The number of independent components (median [25th, 75th]) removed were: 3 [2, 4] for the baseline epochs, 1 [1, 2] for the loss of consciousness epochs, 0 [0, 0] for the maintenance epochs, 2 [1, 4] for the emergence epochs, and 4 [2, 5] for the recovery epochs.

To examine connectivity patterns across the perioperative period (as further described below), electroencephalographic recordings were subjected to the following step to detect and reject noisy data segments. The signals were divided into 2-s windows, and the 2-s data were rejected if (1) the average amplitude was greater than 10 times the average amplitude (or its SD was greater than three times the SD value) of the whole recording, and (2) the above

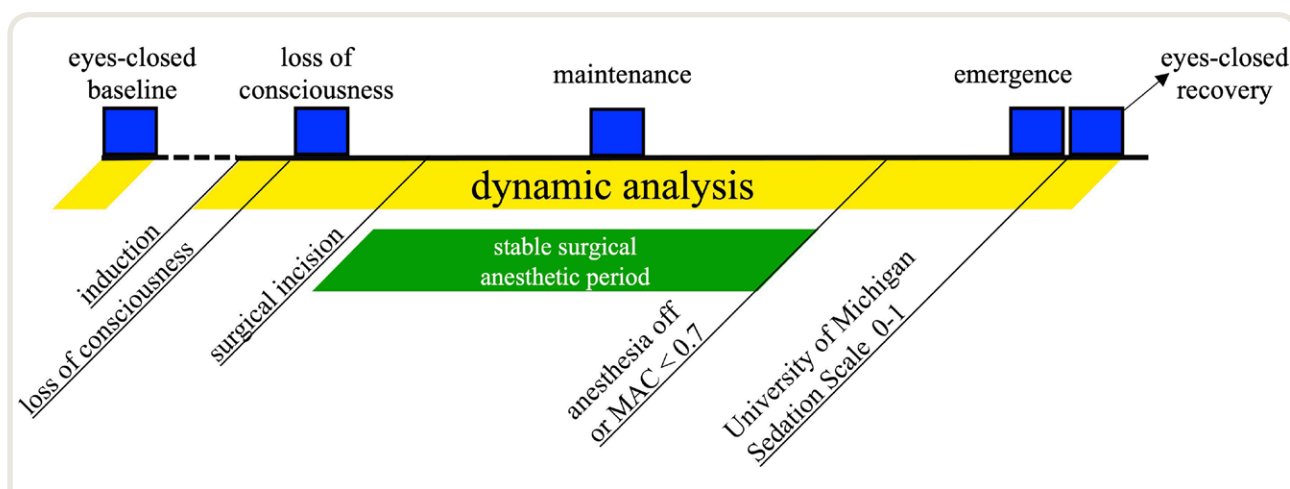


Fig. 1. Study paradigm and electroencephalogram epochs extracted for analysis. Blue squares represent epochs extracted for connectivity analysis. Yellow parallelograms represent the dynamic connectivity analysis periods. The green parallelogram represents the stable surgical anesthetic period (30 s after surgical incision to anesthetic maintenance agent cessation or when the minimum alveolar concentrations fell less than 0.7). MAC, minimum alveolar concentration.

was present in at least 4 of the 16 channels. This step was performed for the induction ($n = 48$), general anesthesia ($n = 49$), and emergence periods ($n = 45$) separately (median [25th, 75th]); 0 [0, 0] %, 3.69 [2.03, 7.16] %, and 9.54 [4.15, 21.25] % of the data were rejected, respectively.

Quantification of Burst Suppression

Burst suppression was identified and quantified as previously described.⁸ In brief, burst suppression was detected based on instantaneous power at 5 to 30 Hz followed by application of a threshold calculated from the manually labeled suppression period yielding a binary series of bursts and suppression states. The suppression ratio was then calculated as a percentage of suppression time in each 60-s binary series (50-s overlap). Because burst suppression confounds the estimation of functional cortical connectivity (described in the next section), time windows with a suppression ratio of greater than 20% were excluded.

Estimation of Functional Connectivity

Cortical functional connectivity was estimated using a weighted phase lag index, which is a measure of the phase synchronization of two signals.¹⁷ It is relatively resistant to the effects of volume conduction and reference montage by accounting for only nonzero phase lead/lag relationships.^{17,18} If the phase of signal consistently leads or lags that of another signal, they are considered phase-locked, and the weighted phase lag index equals 1. Conversely, if the phase relationship is random, the weighted phase lag index would be low. If there is no phase difference, the value will be 0.

As previously described, electroencephalographic signals were divided into 60-s windows with a step size of 10 s and then subdivided into 2-s nonoverlapping subwindows.^{7,8} For each subwindow, the cross-spectral density was estimated using the multitaper method (time-band width product = 2; number of tapers = 3; spectral resolution = 2 Hz) in the Chronux analysis toolbox,¹⁶ and from these repetitions, we estimated the weighted phase lag index as a function of frequency between each pair of channels using a custom-written function adapted from the Fieldtrip toolbox.¹⁹ To attempt to control for spurious connectivity with the weighted phase lag index measure, surrogate data were generated by random shuffling the index of one time series while keeping the other signal unchanged. The cross-spectrum and weighted phase lag index of these shuffled data pairs was subtracted from the original weighted phase lag index to produce the final estimate of functional connectivity.

For this study, we focused on three cortical connectivity regions of interest (prefrontal–frontal [Fp1, Fp2, F5, F6, Fz], frontal–parietal [F5, F6, Fz, P5, P6, Pz], and parietal–occipital [P5, P6, Pz, O1, O2]) due to past studies indicating a role in anesthetic-induced unconsciousness.^{5,7,8,20–22} Connectivity was calculated between individual pairs of channels in these

regions and then averaged for the delta (0.5 to 3 Hz), theta (3 to 7 Hz), and alpha (7 to 13 Hz) frequency bands. The data were then averaged across all time windows in each studied epoch for each participant.

Dynamic Connectivity Analysis

For the preprocessed data across the perioperative period, together with those during baseline and recovery in each participant, the frequency-resolved prefrontal–frontal, frontal–parietal, and parietal–occipital weighted phase lag index was estimated at each 60-s window with a step size of 10 s. The connectivity pattern obtained was a 210-dimensional vector that resulted from 70 frequency estimates for 0.5 to 35 Hz (0.5 Hz step) across three regions. These data were then aggregated across all participants and subjected to principal component analysis. This analysis method uses the covariance structure of the variables to identify mutually orthogonal directions (*i.e.*, principal components) for which most fluctuations occur. Using principal component analysis, we reduced the original 210-dimensional pattern into M -dimensional features while maximally preserving the variance of the original connectivity pattern. The M -dimensional connectivity features were further classified into N_c clusters using k -means clustering algorithm with squared Euclidean distance with 100 replications of the initial centroid. For this study, the number of clusters (N_c) and retained principal components (M) were determined by the stability index, which quantifies the reproducibility of clustering solutions (smaller number suggests higher agreement; mean across 100 realizations),^{23,24} the explained variance by the retained components, and the interpretability of the clustering solutions (Supplemental Digital Content 1, fig. S1, <http://links.lww.com/ALN/C847>).

The cluster analysis partitioned each non-burst suppression time window into one of the N_c clusters. Each cluster can be regarded as a connectivity state that is characterized by distinct spectral and spatial properties. Based on the squared Euclidean distance with these characterized patterns, each time window can be assigned a unique state label; for the windows with burst suppression, we classified them into an additional state as “burst suppression.” The connectivity state time series for consecutive time windows for each participant was thus obtained, which represents the evolution of connectivity states during anesthetic-mediated perturbations of consciousness. We quantified the occurrence rate of each connectivity state, which is defined as the fraction of time spent in that state, for baseline, induction, anesthesia, emergence, and recovery, respectively. Furthermore, to assess how cortical connectivity shifts over time, we calculated the distribution of participants across the $N_c + 1$ states (*i.e.*, the percentage of participants in each state) at each time window, by rescaling the time spans during baseline, induction, general anesthesia (from loss of consciousness to the discontinuation of

anesthetic maintenance agent), emergence, and recovery across all participants.

Temporal Variation in Cortical Connectivity during Stable Surgical Anesthesia

We further employed an alternative method to quantify the temporal variability of the dominant cortical connectivity patterns during the stable surgical anesthesia period and assessed its relationship with participant age (rounded to year). The stable surgical anesthesia period was defined as starting 30 s after skin incision to the cessation of anesthetic maintenance agent or when terminal minimum alveolar concentration values fell to less than 0.7 toward the end of surgery. We chose this minimum alveolar concentration value for the purposes of consistency and comparison with our previous study in adults,⁷ and because it is a clinically relevant lower limit of surgical anesthesia for preventing intraoperative awareness with explicit recall.²⁵ As demonstrated in epoch analysis results, connectivity was dominant in the prefrontal–frontal (2 to 6.5 Hz and 7 to 13 Hz) and frontal–parietal (7 to 13 Hz) regions. For each pattern, we averaged the weighted phase lag index values over the corresponding frequency band for each time window and then calculated the coefficient of variation (defined as the ratio of the SD to the mean) of the values over all available time windows for each participant.

Statistical Analysis

No *a priori* statistical power calculation was performed for sample size estimation. Previous studies that successfully investigated dynamic cortical connectivity in adult surgical patients⁷ as well as healthy volunteers⁸ were used to justify the targeted enrollment.

The data were tested for normality of distribution by Lilliefors corrected Kolmogorov–Smirnov tests. As the null hypothesis of normality of distribution was rejected in some of the data sets ($P < 0.05$), a two-tailed Wilcoxon signed rank test was used to compare the electroencephalogram measure, the weighted phase lag index (median [25th, 75th]) across study epochs, with Bonferroni correction; $P < 0.05/4$ (4 pairs) was considered statistically significant. Pearson correlation was used to measure the similarity of the connectivity patterns between clusters.

Patient characteristics were summarized using means and standard deviations for continuous variables and counts and percentages for categorical variables. Univariate linear regressions were used to assess the association of age and the coefficient of variation of minimum alveolar concentration each with the weighted phase lag index. Then, the same values were used in a multivariable linear regression with weighted phase lag index as the dependent variable and both age and coefficient of variation of minimum alveolar concentration as the independent variables. This enabled quantification of the association between age

and the coefficient of variation of the weighted phase lag index while controlling for minimum alveolar concentration. Goodness of fit was assessed using R^2 . Statistical analyses were performed using SPSS version 26, MATLAB, and R version 4.0.4 (R Core Team [2021]. R: A language and environment for statistical computing. R Foundation for Statistical Computing, Vienna, Austria).

Results

As previously reported, 50 participants completed the study.¹² In total, 175 children were screened for eligibility, 36 declined participation, 52 were excluded due to operative time change or time constraints, 37 were enrolled in another study, 21 were excluded due to research staff availability, 10 due to cancellation or no show for surgery, 3 due to change in the anesthetic plan, and 2 due to technical complications. Participant, anesthetic, and surgical characteristics are presented in table 1. Five participants had incomplete data for race.

Table 1. Participant Characteristics

Participant Characteristics (n = 50)	Values
Age, yr (mean \pm SD)	12.5 \pm 2.4
Age, n (%)	
8–10 yr	15 (30)
11–13 yr	21 (42)
14–16 yr	14 (28)
Female sex, n (%)	21 (42)
Race, n (%)	
White	41 (82)
Black or African American	4 (8)
Other/unknown	5 (10)
Anesthetic duration, min (mean \pm SD)	85 \pm 44.7
Age-adjusted MAC (mean \pm SD)	
Maintenance epoch	1.26 \pm 0.35
Stable surgical anesthetic period	1.24 \pm 0.27
Induction type, n (%)	
Mask (mean age 11 yr)	30 (60)
IV (mean age 13 yr)	20 (40)
Maintenance agent, n (%)	
Sevoflurane	24 (48)
Sevoflurane + nitrous oxide	5 (10)
Isoflurane	15 (30)
Isoflurane + nitrous oxide	6 (12)
Intraoperative opioid administration, n (%)	
Morphine	13 (26)
Fentanyl	48 (96)
IV morphine equivalents (mg/kg)*	0.13 \pm 0.07
Surgical type, n (%)	
Orthopedic	25 (50)
Urology	14 (28)
General	10 (20)
Gynecology	1 (2)

*For intraoperative morphine equivalent calculation, 100 μ g fentanyl = 8 mg morphine. IV, intravenous; MAC, minimum alveolar concentration.

Cortical Connectivity across the Perioperative Period

Group-level averaged functional connectivity using weighted phase lag index values between prefrontal–frontal, frontal–parietal, and parietal–occipital regions across baseline, loss of consciousness, maintenance, emergence, and recovery epochs are shown in figures 2 and 3A (topographical representation). Analysis of region-specific changes is shown in figure 3B and table 2. In the prefrontal–frontal region, significant increases in weighted phase lag index in the delta, theta, and alpha frequency bands were found with loss of consciousness, maintenance, and emergence epochs compared to baseline (table 2; Wilcoxon signed rank test with Bonferroni correction for four pairs comparison). In the recovery epoch, functional connectivity in the delta, theta, and alpha frequency bands returned to baseline levels (table 2). In the frontal–parietal region, there was a significant increase in delta connectivity with loss of consciousness, increase in theta connectivity with maintenance, and decreased alpha connectivity with loss of consciousness (table 2). In the parietal–occipital region, a significant increase in connectivity in delta with loss of consciousness, and reductions across all epochs were found with the alpha frequency band (table 2). Additional analyses of these data without removal of segments contaminated by artifacts (*i.e.*, cardiac, eye, and/or movement artifact[s]) were consistent with the reported results (data not shown).

Dynamic Patterns of Cortical Connectivity across the Perioperative Period

To investigate the temporal dynamics of connectivity patterns across the perioperative period in subjects at the group level using frequency resolved weighted phase lag index, k-means cluster analysis was used. Multiple cluster solutions were tested. The seven-cluster solution was selected (1) because this was the best solution when accounting for the reproducibility of the clustering results (stability index; Supplemental Digital Content 1, fig. S1, <http://links.lww.com/ALN/C847>) and (2) because of the empirical observation that the dominant connectivity characteristics during baseline are different than general anesthesia (fig. 2). For the 7-cluster solution, when the first 39 principal components were retained, 90.13% of the variance was contained. The characteristics of the identified clusters (connectivity states) are described in table 3 and shown in figure 4A. The identified clusters demonstrated distinct differences across states of consciousness (*e.g.*, cluster 1 *vs.* 4 representing the eyes closed baseline/recovery *vs.* emergence period, respectively; fig. 4C), but constrained diversity patterns were found during the maintenance phase of general anesthesia (*i.e.*, clusters 5 to 7), with a between-cluster correlation of 0.851 for cluster 5 *versus* 6, 0.868 for cluster 6 *versus* 7, and 0.748 for cluster 5 *versus* 7 (Pearson correlation; fig. 4B). Due to the strong similarity of cluster patterns found in the

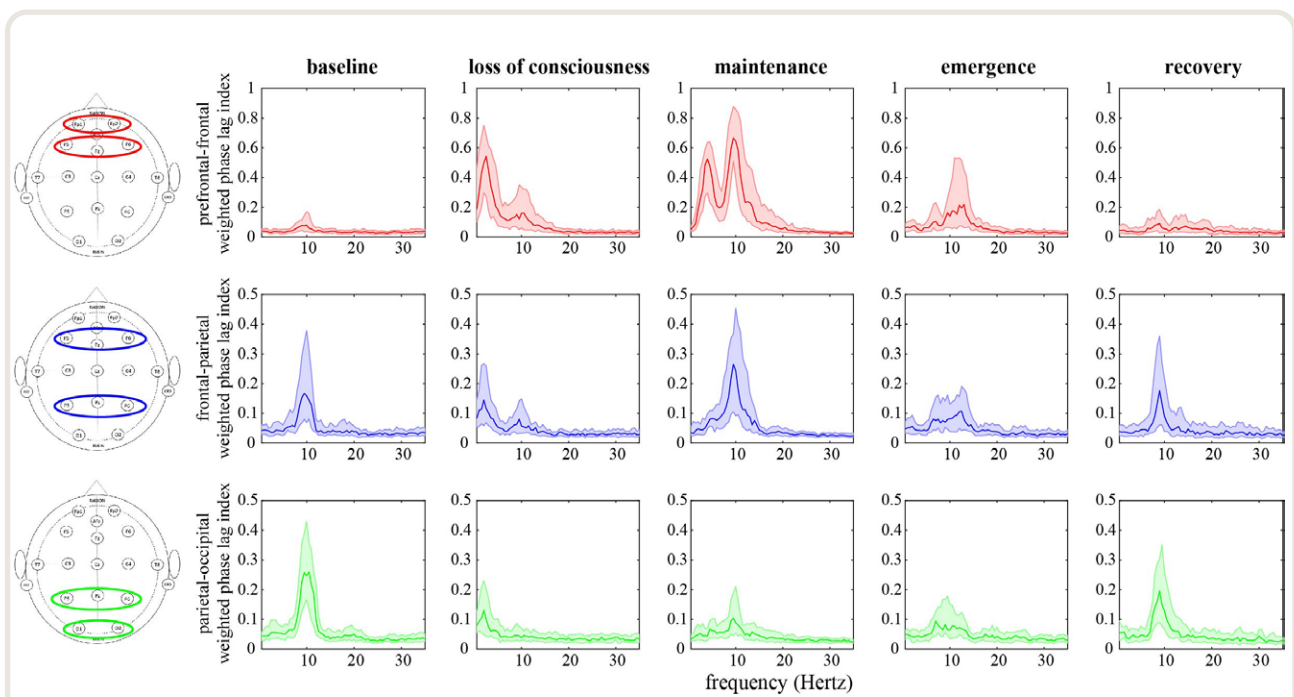


Fig. 2. Functional connectivity measured using weighted phase lag index values between the prefrontal–frontal (red), frontal–parietal (blue), and parietal–occipital (green) regions across baseline ($n = 50$), loss of consciousness ($n = 50$), maintenance ($n = 49$), emergence ($n = 45$), and recovery epochs ($n = 45$). In each, the bold line represents the median, and the shaded area indicates the 25th and 75th percentiles across subjects for each period and region.

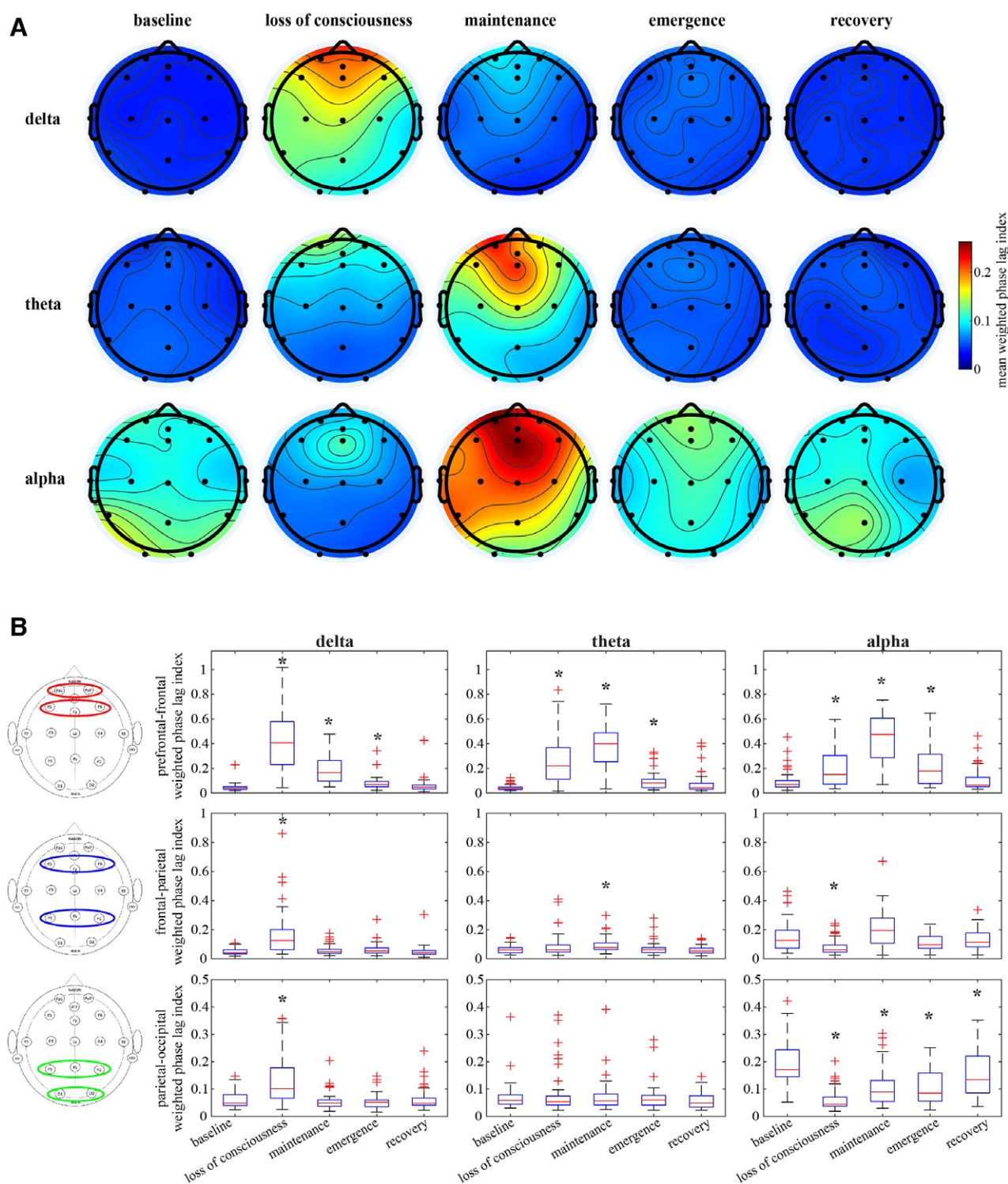


Fig. 3. Group-level topography of functional connectivity strength using mean weighted phase lag index in each channel (*black dot*) across all other channels (*A*) and in the prefrontal–frontal (*red*), frontal–parietal (*blue*), and parietal–occipital (*green*) regions for the delta, theta, and alpha frequency bands across analysis epochs (*B*). The *central marks* in the *boxes* represent the median values, with the *edges* representing the 25th and 75th percentiles. The *extending whiskers* are the most extreme data points determined by the MATLAB algorithm (version R2019b; MathWorks, Inc., USA) to be nonoutliers, and the *red crosses* are those values deemed to be outliers. The *asterisks* denote significance using the Wilcoxon signed rank test with Bonferroni correction ($P < 0.05/4$ for four-pair comparison).

Table 2. Weighted Phase Lag Index Values in Different Regions of the Brain

Frequency and Brain Region		Perioperative Epoch			
	Baseline	Loss of Consciousness	Maintenance	Emergence	Recovery
Delta					
Prefrontal–frontal	0.041 [0.030, 0.052]	0.407 [0.232, 0.578], $P < 0.001^*$	0.166 [0.097, 0.264], $P < 0.001^*$	0.070 [0.052, 0.095], $P < 0.001^*$	0.048 [0.033, 0.067], $P = 0.038$
Frontal–parietal	0.041 [0.034, 0.061]	0.125 [0.062, 0.201], $P < 0.001^*$	0.048 [0.037, 0.064], $P = 0.092$	0.053 [0.038, 0.073], $P = 0.042$	0.041 [0.030, 0.056], $P = 0.870$
Parietal–occipital	0.049 [0.040, 0.080]	0.101 [0.066, 0.178], $P < 0.001^*$	0.050 [0.037, 0.061], $P = 0.442$	0.052 [0.036, 0.061], $P = 0.413$	0.049 [0.041, 0.067], $P = 0.942$
Theta					
Prefrontal–frontal	0.038 [0.029, 0.048]	0.222 [0.112, 0.369], $P < 0.001^*$	0.399 [0.254, 0.488], $P < 0.001^*$	0.081 [0.045, 0.112], $P < 0.001^*$	0.045 [0.031, 0.080], $P = 0.044$
Frontal–parietal	0.059 [0.039, 0.076]	0.060 [0.045, 0.095], $P = 0.212$	0.077 [0.063, 0.109], $P < 0.001^*$	0.061 [0.041, 0.076], $P = 0.474$	0.052 [0.038, 0.072], $P = 0.474$
Parietal–occipital	0.059 [0.045, 0.079]	0.054 [0.042, 0.075], $P = 0.792$	0.057 [0.042, 0.083], $P = 0.751$	0.060 [0.041, 0.077], $P = 0.504$	0.050 [0.034, 0.076], $P = 0.077$
Alpha					
Prefrontal–frontal	0.070 [0.049, 0.101]	0.151 [0.071, 0.305], $P < 0.001^*$	0.474 [0.286, 0.606], $P < 0.001^*$	0.178 [0.078, 0.315], $P < 0.001^*$	0.066 [0.053, 0.128], $P = 0.453$
Frontal–parietal	0.126 [0.072, 0.196]	0.060 [0.045, 0.095], $P < 0.001^*$	0.194 [0.106, 0.279], $P = 0.036$	0.096 [0.071, 0.154], $P = 0.014$	0.114 [0.081, 0.178], $P = 0.167$
Parietal–occipital	0.171 [0.145, 0.243]	0.044 [0.038, 0.071], $P < 0.001^*$	0.089 [0.055, 0.132], $P < 0.001^*$	0.085 [0.056, 0.159], $P < 0.001^*$	0.135 [0.086, 0.221], $P = 0.003^*$
Shown are the weighted phase lag index values across perioperative epochs for the prefrontal–frontal, frontal–parietal, and parietal–occipital brain regions in the delta, theta, and alpha frequency bands. Analysis was performed with the Wilcoxon signed rank test with Bonferroni correction for four pairs comparison. The values are shown as the median [25th, 75th].					
* $P < 0.05/4$, which was considered statistically significant.					

Shown are the weighted phase lag index values across perioperative epochs for the prefrontal–frontal, frontal–parietal, and parietal–occipital brain regions in the delta, theta, and alpha frequency bands. Analysis was performed with the Wilcoxon signed rank test with Bonferroni correction for four pairs comparison. The values are shown as the median [25th, 75th].

* $P < 0.05/4$, which was considered statistically significant.

developing brain during the surgical stable period and limitations of cluster analysis (*i.e.*, possibility of forced clustering with similar data), we were unable to further investigate dynamic transition characteristics in connectivity patterns during this period nor test for an association with age.

Age-related Changes in Temporal Connectivity during the Stable Surgical Anesthesia Period

Using an alternative *post hoc* approach to address age-related temporal changes in functional connectivity during the stable surgical anesthetic period, we investigated the temporal variations in weighted phase lag index values as a function of age. Using the three prominent connectivity bands (prefrontal–frontal 2 to 6.5 and 7 to 13 Hz; and frontal–parietal 7 to 13 Hz; representative connectograms are shown in Supplemental Digital Content 1, fig. S2, <http://links.lww.com/ALN/C847>), we measured the coefficient of variation of the weighted phase lag index as a function of age while controlling for changes in minimum alveolar concentration values during the surgical stable anesthetic period (multivariable analysis). A significant association of the coefficient of variation in weighted phase lag index and age was found for the prefrontal–frontal 2 to 6.5 Hz connectivity band (slope = 0.02, $P = 0.007$, $R^2 = 0.34$) but not for the prefrontal–frontal 7 to 13 Hz band (0.01, $P = 0.209$, $R^2 = 0.14$) or the frontal–parietal 7 to 13 Hz band (0.02, $P = 0.053$, $R^2 = 0.10$; fig. 5). Additional analyses of the association of age and the coefficient of variation for the weighted phase lag index (across the three prominent connectivity bands) while controlling for the average intraoperative minimum alveolar concentration values or intraoperative morphine equivalent administration were relatively consistent with the findings above; however, maintenance of general anesthesia supplemented with nitrous oxide was associated with an increased coefficient of variation of the weighted phase lag index (Supplemental Digital Content 1, fig. S3, <http://links.lww.com/ALN/C847>).

Discussion

This study demonstrated that general anesthesia in children correlates with changes in functional connectivity patterns but, unlike in adults, functional connectivity changes appear stable rather than dynamic. Specifically, during the maintenance phase of general anesthesia, connectivity patterns were consistently dominated by theta and alpha prefrontal–frontal and alpha frontal–parietal connectivity, which exhibited high between-pattern similarity. Additional *post hoc* investigation of temporal changes in connectivity patterns suggests the possibility of age-dependent increases in connectivity variations (*i.e.*, age-dependent increase in the temporal variation of prefrontal–frontal theta connectivity). Overall, these data support the hypothesis that during the stable maintenance phase of general anesthesia, functional connectivity

Table 3. Characteristics of Connectivity States across the Perioperative Period

Connectivity State	Dominant Frequency Range	Predominant Region	Predominant Associated Conscious State
1	7 to 13 Hz	Prefrontal–frontal, frontal–parietal, parietal–occipital	Baseline and recovery
2	—	—	Induction and emergence
3	2 to 6 Hz	Prefrontal–frontal	After loss of consciousness
4	7 to 13 Hz	Prefrontal–frontal	Emergence
5	2 to 6 and 7 to 13 Hz	Prefrontal–frontal	Maintenance
6	2 to 6 and 7 to 13 Hz	Prefrontal–frontal	Maintenance
7	2 to 6 and 7 to 13 Hz	Prefrontal–frontal, and frontal–parietal (7 to 13 Hz only)	Maintenance
Burst suppression	—	—	After loss of consciousness

patterns in the developing brain are constrained, in contrast to the structured transitions (both bandwidth and region specific) previously shown in adults.^{7,8}

We first investigated changes in functional connectivity using the conventionally defined time epochs (*i.e.*, static analysis) across anesthetic-mediated changes in states of consciousness. Consistent with what has been shown in animal models and adult subjects, we found a breakdown in frontal–parietal alpha functional connectivity with the loss of consciousness but return during the maintenance and emergence periods.^{26,27} This finding supports the conclusion of Vlisides *et al.*⁷ that a single measure of frontal–parietal functional connectivity is likely insufficient to reflect surgical anesthetic levels. However, we observed a hyperconnected frontal cortex during the loss of consciousness, maintenance, and emergence periods (across the delta, theta, and alpha frequencies),^{7,28,29} which may reflect thalamocortical hyper-synchronization previously shown to occur with γ -aminobutyric acid-mediated (GABAergic) anesthetic agents.³⁰

To address dynamic changes in functional connectivity across the perioperative period, we applied a cluster analysis method (k-means) and identified functional connectivity patterns (clusters) associated with the various perioperative/anesthetic states. The associated cluster during the baseline and recovery periods in the eyes-closed resting state demonstrated predominant alpha connectivity across all three regions tested (prefrontal–frontal, frontal–parietal, and parietal–occipital), which parallels findings in our complementary study in adults.⁸ Although the significance of alpha oscillation synchronization in neuronal networks is still under investigation, evidence supports both an inhibitory and task-relevant role in neuronal processing.^{31,32} The similarity in connectivity states found in this study of pediatric subjects compared to what was previously shown in adults may reflect developmental milestones that are already achieved (*e.g.*, modulation of neural network activity, sensory integration, and/or perception).^{8,31,33} Considering this possible functional role, in addition to empirical evidence supporting posterior alpha oscillations as a potential surrogate of the conscious state (*i.e.*, anteriorization with unconsciousness and slow gradual return with recovery),^{32,34} it is not surprising that these connectivity pattern

clusters are associated with the baseline and recovery states. However, contrary to our hypothesis, we were not able to further investigate dynamic transition characteristics during the stable maintenance phase of general anesthesia because certain connectivity patterns (*i.e.*, clusters 5, 6, and 7) exhibited high between-cluster correlations. This is in contrast to what was found in both a pragmatic surgical setting and a rigorously controlled anesthetic exposure paradigm in younger adults not undergoing surgery.^{7,8} Both of these studies in adults found a diversity of distinct connectivity patterns that toggled between connectivity states in a structured manner.^{7,8} Additionally, beyond the lack of distinct connectivity patterns during general anesthesia in this developmental period, clusters displayed more regional congruence (*i.e.*, strong alpha connectivity in both the prefrontal–frontal region as well as the frontal–parietal region) as well as bandwidth overlap (*i.e.*, strong prefrontal–frontal theta and alpha connectivity; fig. 4A).

The constrained or restricted repertoire of connectivity patterns found in this study highlights an important functional neural network difference during this developmental period. This finding is further supported by the pragmatic setting in which this study was conducted. Despite limiting the maintenance anesthetic agent to a halogenated ether, there were clinical variations in minimum alveolar concentrations used for the maintenance phase of general anesthesia as well as nitrous oxide supplementation in some subjects, yet connectivity patterns were remarkably similar across the study cohort. In terms of a biologically plausible explanation, first consider the hypothesis that the brain is a dynamical system that exists in multiple metastable states.³⁵ This is often conceptually described as an energy landscape using a ball and well model, where the wells represent states and the hills between them represent the energy barriers to transition between these states.³⁵ Applying this hypothetical model to our findings of children undergoing general anesthesia, it may be that the restricted states (and/or restricted transitions) are attributable to an immature structural and functional architecture that results in either the increase in the energy barrier required for transition (*i.e.*, deeper well), or a decrease in the number of metastable states during general anesthesia (*i.e.*, decreased number of wells). Although

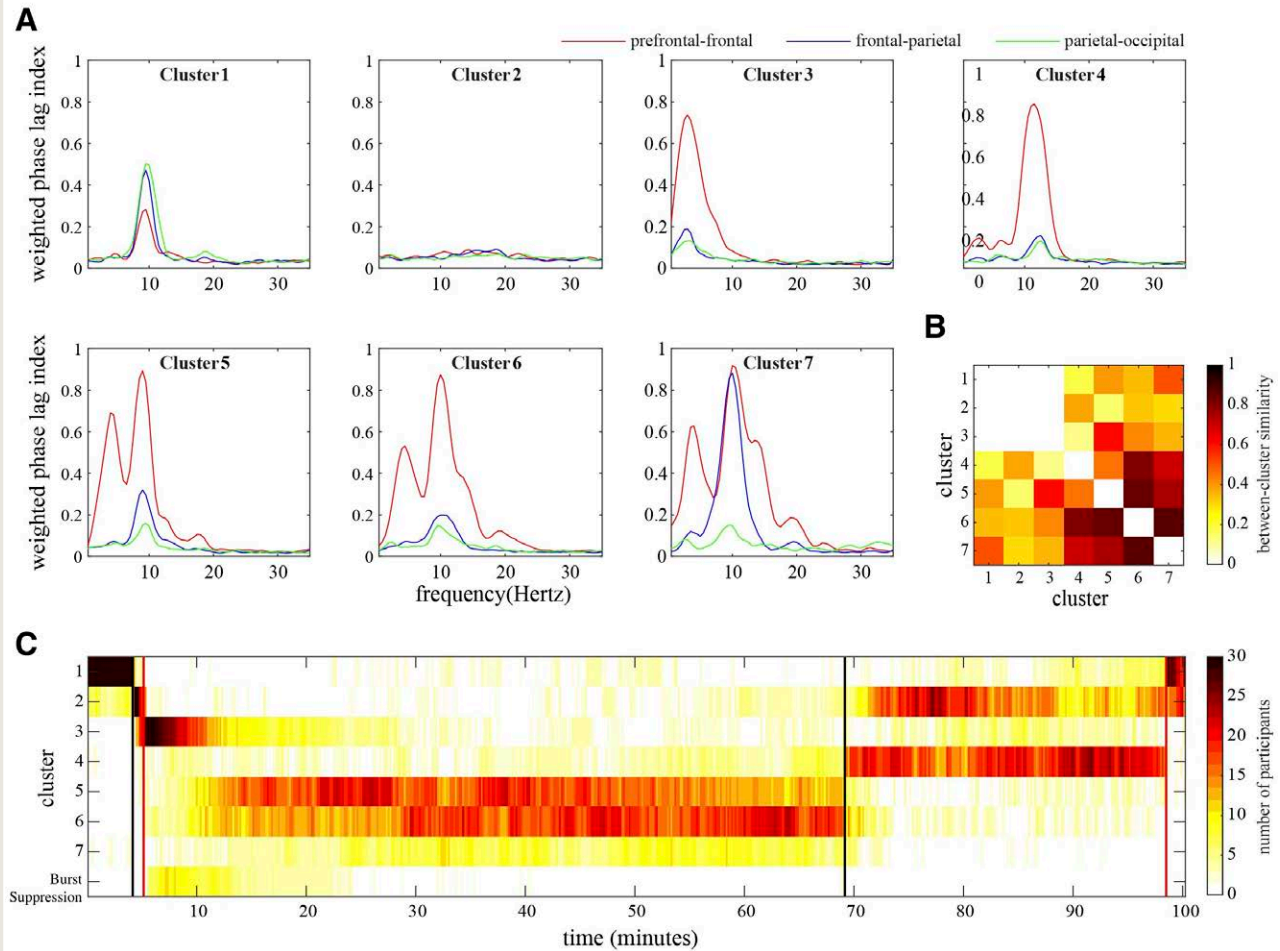


Fig. 4. Dynamic cortical connectivity across the perioperative period. (A) Representative connectivity patterns for each cluster/connec-tivity state measured using the weighted phase lag index. *Red*, prefrontal–frontal; *blue*, frontal–parietal; *green*, parietal–occipital. (B) The between-cluster similarity for each pair of clusters/connec-tivity states. (C) The temporal progression of the distribution of the participants across clusters/connec-tivity states (i.e., percentage of participants in each state). (Left to right) The left-hand black vertical line indicates the start of induction that separates the baseline and induction periods, the left-hand red line indicates the time when loss of consciousness occurred, the right-hand black line indicates the discontinuation of anesthetic maintenance agent (or minimum alveolar concentration less than 0.7), and the right-hand red line indicates recovery of consciousness that separates the emergence and recovery periods. The time spans during baseline ($n = 50$), induction ($n = 48$), maintenance ($n = 49$), emergence ($n = 45$), and recovery ($n = 45$) were rescaled before the calculation.

the neurobiological mechanism(s) that account for these findings remain speculative, the transition from childhood to adulthood is marked by a general increase in functional integration,³⁶ increased neural signal complexity,^{12,37,38} and brain signal variability.³⁹ Moreover, this period is associated with a transition from stronger short-range connections to stronger long-range connections, as well as progression in hierarchical organization.^{13,41–42} A recent comparative study of children (8 to 15 yr) *versus* young adults (20 to 33 yr) undergoing a face memory task demonstrated that brain maturation was associated with greater brain signal

variability and task performance, as well as reduced response time.³⁹ Another comparative study of children (7 to 9 yr *vs.* 19 to 22 yr) demonstrated increased strength of long-range functional connectivity and increased corticocortical connectivity with maturation.⁴² Further, there is evidence to suggest that constrained connectivity patterns may be a developmental effect. In a study examining dynamic transition probabilities of functional connectivity states during surgical anesthesia in adult subjects, there was no correlation with age.¹⁰ Collectively, our data, interpreted in the context of these developmental findings, support the hypothesis

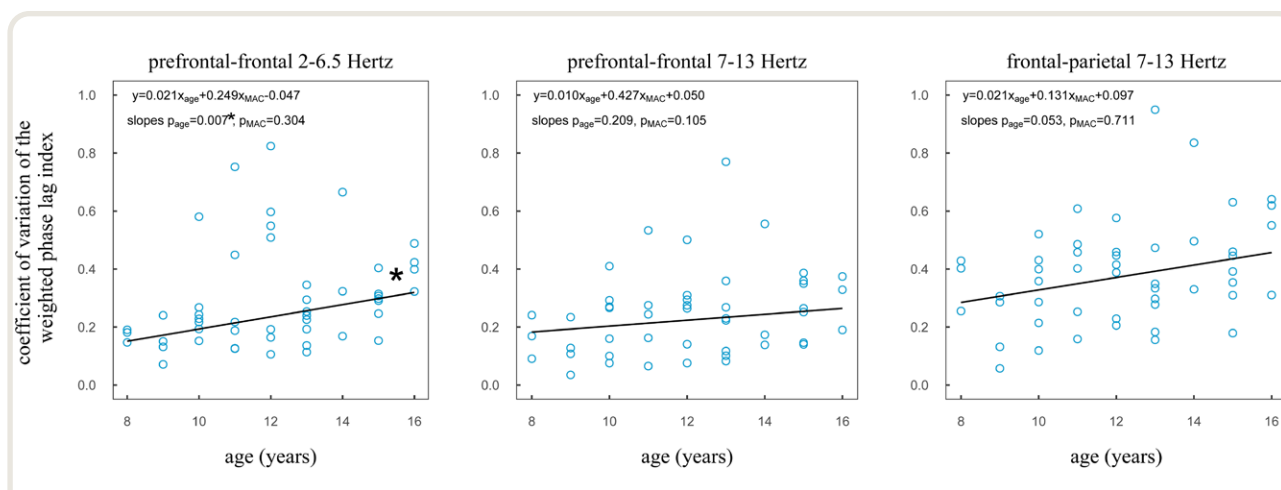


Fig. 5. Association of age and temporal variations in the three dominant connectivity patterns during the stable surgical anesthesia period. Multivariable linear regression assessing the association of age and coefficient of variation for the weighted phase lag index controlling for changes in the minimum alveolar concentration (MAC) in the prefrontal–frontal 2 to 6.5 Hz (*left*), prefrontal–frontal 7 to 13 Hz (*middle*), and frontal–parietal 7 to 13 Hz (*right*) bands. The *line* is plotted at the mean coefficient of variation of the minimum alveolar concentration value, 0.120. The line equation and *P* values for slopes (age and coefficient of variation of minimum alveolar concentration) are shown in the *upper left corner* of each connectivity band. The *asterisk* denotes statistical significance ($P < 0.05$).

that brain network development undergoes an evolution of connectivity states in which maturation is associated with increased diversity (or access) and measurable during general anesthesia. However, additional studies are required to fully support this interpretation.

Due to the cluster similarity during the maintenance of general anesthesia, we were unable to test for the association of age and functional connectivity “state” transitions. As an alternative approach, our *post hoc* analysis of the variation in the weighted phase lag index during general anesthesia with age indicated that an effect may be present in some (*e.g.*, prefrontal–frontal 2 to 6.5 Hz band) but not all connectivity bands and potentially influenced by supplementation with nitrous oxide. Although this finding is preliminary, it is consistent with the increased neural oscillatory diversity and network development discussed above. It is also generally supported by our findings of increased baseline cortical complexity (measured before any drug administration) with age in this same cohort of children, but understanding the relationship between baseline dynamics and how they covary with functional measures of connectivity during general anesthesia remains an open question.¹²

Limitations

There are several limitations to consider when interpreting these findings. First, this was a pragmatic study in children undergoing surgery and general anesthesia and thus has the potential for the presence of selection bias (*i.e.*, convenience sampling); however, we attempted to address this using a prespecified stratified recruitment paradigm representative of our regional population. Additionally, although we used

study enrollment and analysis criteria to control for anesthetic type, induction method, maintenance agent, and minimum alveolar concentration values, clinical variations in anesthetic minimum alveolar concentration as well as supplementation with nitrous oxide occurred in some children. Despite this variability, constrained connectivity patterns were found, which further supports our state-specific interpretation of these data. Second, behavioral responses during the loss of consciousness with the induction of general anesthesia were clinically assessed by the anesthesia provider without behavioral testing, thus limiting timing precision. Third, electroencephalogram data were collected with a relatively low channel density (*i.e.*, 16 channels), limiting resolution. Fourth, the analysis method, the weighted phase lag index, lacks directionality of the functional connection but is relatively resistant to the effects of volume conduction and reference montage by accounting for only nonzero phase lead/lag relationships, which supports our rationale for use in the current study with limited channel numbers.^{17,18} Fifth, following our adult studies, the *k*-means algorithm was used for the clustering analysis, which partitioned the connectivity during anesthesia into different clusters (clusters 5 to 7), although they are characterized by similar spectral and regional properties. The integration of hierarchical clustering or probabilistic clustering may improve the clustering performance. Sixth, the analysis of the association of temporal variation in functional connectivity with age was performed *post hoc* and thus should be considered exploratory. Last, this study was performed in the real-world perioperative space. Although this study design confers external validity, confounding factors such as anxiety, errant noises during baseline recordings, among others, were possible.

Conclusions

Our results suggest that, unlike functional connectivity patterns in adults, those recorded during late childhood and early adolescence are more stable during general anesthesia. We also provide further evidence that a single measure of frontal–parietal functional connectivity is likely to be inadequate as a reliable neural correlate of surgical anesthesia but support previous findings of a hyperconnected frontal cortex during general anesthesia. These data contribute to the growing body of knowledge of developmental neurobiology and inform the advancement of monitoring strategies of the immature brain during the perioperative period.

Acknowledgments

The authors thank the children and their families for their participation in this study.

Research Support

Supported by Foundation for Anesthesia Education and Research (Schaumburg, Illinois) grant No. 20–PAF00823, the National Institute of Health (Bethesda, Maryland) grant No. K23GM126317, and by the Department of Anesthesiology, University of Michigan Medical School, Ann Arbor, Michigan.

Competing Interests

Dr. Mashour is a consultant for TRYP Therapeutics (San Diego, California). Dr. Vlisides receives support from Blue Cross Blue Shield of Michigan (Detroit, Michigan) for delirium quality improvement initiatives unrelated to this work. The other authors declare no competing interests.

Correspondence

Address correspondence to Dr. Puglia: 4-911 Mott Hospital, 1540 E. Hospital Dr., SPC 4245, Ann Arbor, Michigan 48109-4245. mpuglia@med.umich.edu. This article may be accessed for personal use at no charge through the Journal Web site, www.anesthesiology.org.

References

1. Rabbitts JA, Groenewald CB: Epidemiology of pediatric surgery in the United States. *Paediatr Anaesth* 2020; 30:1083–90
2. Boly M, Moran R, Murphy M, Boveroux P, Bruno MA, Noirhomme Q, Ledoux D, Bonhomme V, Brichant JF, Tononi G, Laureys S, Friston K: Connectivity changes underlying spectral EEG changes during propofol-induced loss of consciousness. *J Neurosci* 2012; 32:7082–90
3. Lee U, Kim S, Noh GJ, Choi BM, Hwang E, Mashour GA: The directionality and functional organization of frontoparietal connectivity during consciousness and anesthesia in humans. *Conscious Cogn* 2009; 18:1069–78
4. Pappas I, Cornelissen L, Menon DK, Berde CB, Stamatakis EA: δ -Oscillation correlates of anesthesia-induced unconsciousness in large-scale brain networks of human infants. *ANESTHESIOLOGY* 2019; 131:1239–53
5. Hudetz AG, Mashour GA: Disconnecting consciousness: Is there a common anesthetic end point? *Anesth Analg* 2016; 123:1228–40
6. Luppi AI, Craig MM, Pappas I, Finoia P, Williams GB, Allanson J, Pickard JD, Owen AM, Naci L, Menon DK, Stamatakis EA: Consciousness-specific dynamic interactions of brain integration and functional diversity. *Nat Commun* 2019; 10:4616
7. Vlisides PE, Li D, Zierau M, Lapointe AP, Ip KI, McKinney AM, Mashour GA: Dynamic cortical connectivity during general anesthesia in surgical patients. *ANESTHESIOLOGY* 2019; 130:885–97
8. Li D, Vlisides PE, Kelz MB, Avidan MS, Mashour GA; ReCCognition Study Group: Dynamic cortical connectivity during general anesthesia in healthy volunteers. *ANESTHESIOLOGY* 2019; 130:870–84
9. Mashour GA, Roelfsema P, Changeux JP, Dehaene S: Conscious processing and the global neuronal workspace hypothesis. *Neuron* 2020; 105:776–98
10. Li D, Puglia MP, Lapointe AP, Ip KI, Zierau M, McKinney A, Vlisides PE: Age-related changes in cortical connectivity during surgical anesthesia. *Front Aging Neurosci* 2019; 11:371
11. von Elm E, Altman DG, Egger M, Pocock SJ, Gøtzsche PC, Vandenbroucke JP; STROBE Initiative: The Strengthening the Reporting of Observational Studies in Epidemiology (STROBE) statement: Guidelines for reporting observational studies. *J Clin Epidemiol* 2008; 61:344–9
12. Puglia MP, Li D, Leis AM, Jewell ES, Kaplan CM, Therrian M, Kim M, Lee U, Mashour GA, Vlisides PE: Neurophysiologic complexity in children increases with developmental age and is reduced by general anesthesia. *ANESTHESIOLOGY* 2021; 135:813–28
13. Menon V: Developmental pathways to functional brain networks: Emerging principles. *Trends Cogn Sci* 2013; 17:627–40
14. Delorme A, Makeig S: EEGLAB: An open source toolbox for analysis of single-trial EEG dynamics including independent component analysis. *J Neurosci Methods* 2004; 134:9–21
15. Malviya S, Voepel-Lewis T, Tait AR, Merkel S, Tremper K, Naughton N: Depth of sedation in children undergoing computed tomography: Validity and reliability of the University of Michigan Sedation Scale (UMSS). *Br J Anaesth* 2002; 88:241–5
16. Mitra P, Bokil H: *Observed Brain Dynamics*. New York, Oxford University Press, 2008
17. Vinck M, Oostenveld R, van Wingerden M, Battaglia F, Pennartz CM: An improved index of phase-synchronization for electrophysiological data in the presence of volume-conduction, noise and sample-size bias. *Neuroimage* 2011; 55:1548–65

18. Stam CJ, Nolte G, Daffertshofer A: Phase lag index: Assessment of functional connectivity from multi channel EEG and MEG with diminished bias from common sources. *Hum Brain Mapp* 2007; 28:1178–93
19. Oostenveld R, Fries P, Maris E, Schoffelen JM: FieldTrip: Open source software for advanced analysis of MEG, EEG, and invasive electrophysiological data. *Comput Intell Neurosci* 2011; 2011:156869
20. Flores FJ, Hartnack KE, Fath AB, Kim SE, Wilson MA, Brown EN, Purdon PL: Thalamocortical synchronization during induction and emergence from propofol-induced unconsciousness. *Proc Natl Acad Sci U S A* 2017; 114:E6660–8
21. Purdon PL, Pierce ET, Mukamel EA, Prerau MJ, Walsh JL, Wong KF, Salazar-Gomez AF, Harrell PG, Sampson AL, Cimenser A, Ching S, Kopell NJ, Tavares-Stoeckel C, Habeeb K, Merhar R, Brown EN: Electroencephalogram signatures of loss and recovery of consciousness from propofol. *Proc Natl Acad Sci U S A* 2013; 110:E1142–51
22. Cornelissen L, Kim SE, Purdon PL, Brown EN, Berde CB: Age-dependent electroencephalogram (EEG) patterns during sevoflurane general anesthesia in infants. *Elife* 2015; 4:e06513
23. Hudson AE, Calderon DP, Pfaff DW, Proekt A: Recovery of consciousness is mediated by a network of discrete metastable activity states. *Proc Natl Acad Sci U S A* 2014; 111:9283–8
24. Lange T, Roth V, Braun ML, Buhmann JM: Stability-based validation of clustering solutions. *Neural Comput* 2004; 16:1299–323
25. Avidan MS, Jacobsohn E, Glick D, Burnside BA, Zhang L, Villafranca A, Karl L, Kamal S, Torres B, O'Connor M, Evers AS, Gradwohl S, Lin N, Palanca BJ, Mashour GA; BAG-RECALL Research Group: Prevention of intraoperative awareness in a high-risk surgical population. *N Engl J Med* 2011; 365:591–600
26. Lee H, Mashour GA, Noh GJ, Kim S, Lee U: Reconfiguration of network hub structure after propofol-induced unconsciousness. *ANESTHESIOLOGY* 2013; 119:1347–59
27. Uhrig L, Sitt JD, Jacob A, Tasserie J, Barttfeld P, Dupont M, Dehaene S, Jarraya B: Resting-state dynamics as a cortical signature of anesthesia in monkeys. *ANESTHESIOLOGY* 2018; 129:942–58
28. Banks MI, Krause BM, Endemann CM, Campbell DI, Kovach CK, Dyken ME, Kawasaki H, Nourski KV: Cortical functional connectivity indexes arousal state during sleep and anesthesia. *Neuroimage* 2020; 211:116627
29. Kallionpää RE, Valli K, Scheinin A, Långsjö J, Maksimow A, Vahlberg T, Revonsuo A, Scheinin H, Mashour GA, Li D: Alpha band frontal connectivity is a state-specific electroencephalographic correlate of unresponsiveness during exposure to dexmedetomidine and propofol. *Br J Anaesth* 2020; 125:518–28
30. Ching S, Cimenser A, Purdon PL, Brown EN, Kopell NJ: Thalamocortical model for a propofol-induced α -rhythm associated with loss of consciousness. *Proc Natl Acad Sci U S A* 2010; 107: 22665–70
31. Palva S, Palva JM: Functional roles of alpha-band phase synchronization in local and large-scale cortical networks. *Front Psychol* 2011; 2:204
32. Pavone KJ, Su L, Gao L, Eromo E, Vazquez R, Rhee J, Hobbs LE, Ibala R, Demircioglu G, Purdon PL, Brown EN, Akeju O: Lack of responsiveness during the onset and offset of sevoflurane anesthesia is associated with decreased awake-alpha oscillation power. *Front Syst Neurosci* 2017; 11:38
33. Sadaghiani S, Scheeringa R, Lehongre K, Morillon B, Giraud A-L, D'Esposito M, Kleinschmidt A: Alpha-band phase synchrony is related to activity in the fronto-parietal adaptive control network. *J Neurosci* 2012; 32:14305–10
34. Blain-Moraes S, Tarnal V, Vanini G, Bel-Behar T, Janke E, Picton P, Golmirzaie G, Palanca BJA, Avidan MS, Kelz MB, Mashour GA: Network efficiency and posterior alpha patterns are markers of recovery from general anesthesia: A high-density electroencephalography study in healthy volunteers. *Front Hum Neurosci* 2017; 11:328
35. Hudson AE: Metastability of neuronal dynamics during general anesthesia: Time for a change in our assumptions? *Front Neural Circuits* 2017; 11:58
36. Miskovic V, Ma X, Chou CA, Fan M, Owens M, Sayama H, Gibb BE: Developmental changes in spontaneous electrocortical activity and network organization from early to late childhood. *Neuroimage* 2015; 118:237–47
37. Fernández A, Quintero J, Hornero R, Zuluaga P, Navas M, Gómez C, Escudero J, García-Campos N, Biederman J, Ortiz T: Complexity analysis of spontaneous brain activity in attention-deficit/hyperactivity disorder: Diagnostic implications. *Biol Psychiatry* 2009; 65:571–7
38. Fernández A, Zuluaga P, Abásolo D, Gómez C, Serra A, Méndez MA, Hornero R: Brain oscillatory complexity across the life span. *Clin Neurophysiol* 2012; 123:2154–62
39. McIntosh AR, Kovacevic N, Itier RJ: Increased brain signal variability accompanies lower behavioral variability in development. *PLoS Comput Biol* 2008; 4:e1000106
40. Yap QJ, Teh I, Fusar-Poli P, Sum MY, Kuswanto C, Sim K: Tracking cerebral white matter changes across the lifespan: Insights from diffusion tensor imaging studies. *J Neural Transm (Vienna)* 2013; 120:1369–95
41. Grayson DS, Fair DA: Development of large-scale functional networks from birth to adulthood: A guide to the neuroimaging literature. *Neuroimage* 2017; 160:15–31
42. Supekar K, Musen M, Menon V: Development of large-scale functional brain networks in children. *PLoS Biol* 2009; 7:e1000157